Solvent Effects on Vibrational Coherence and Ultrafast Reaction Dynamics in the Multicolor Pump−Probe Spectroscopy of Intervalence Electron Transfer

Patanjali Kambhampati, Dong Hee Son, Tak W. Kee, and Paul F. Barbara*

Department of Chemistry and Biochemistry, The University of Texas at Austin, Austin, Texas 78712

Received: July 18, 2000; In Final Form: September 11, 2000

A detailed investigation of ultrafast photoinduced electron transfer (ET) in a mixed valence compound ($(NH_3)_5RuNCRu(CN)_5^-$; RuRu) in formamide, ethylene glycol, and glycerol was performed using variable wavelength femtosecond pump−probe spectroscopy over a broad range of pump and probe wavelengths. The ET kinetics were monitored by observing recovery of the ground state population. The spectra are highly dynamic, indicating the need for broad spectral coverage to accurately unravel the ET kinetics from excited state and ground state relaxation dynamics. ET is observed to proceed more slowly in slower solvents in a manner consistent with the Hybrid model of solution phase electron transfer. The ET time ($1/e$) of RuRu in ethylene glycol is 220 fs compared to 100 fs in water. As recently reported for RuRu in water, the ET time is pump wavelength independent. A previously unobserved pump wavelength dependence of the early time dynamics, however, is observed which is assigned to stimulated emission prior to vibrational relaxation in the excited state. The early time dynamics of the stimulated emission is solvent dependent as demonstrated by the pump wavelength dependence while probing at the red edge of the static absorption spectra. The oscillatory features observed in the pump−probe signal are assigned to vibrational coherence on the ground electronic state created primarily by resonant impulsive stimulated Raman scattering (RISRS). The dephasing time of the vibrational coherence is solvent dependent as are the vibrational population relaxation rates. The wavelength dependent phase and amplitude of the oscillations show differences from typical RISRS signals, which suggest non-Condon contributions to the oscillations. The solvent dependence of the oscillation amplitude suggests the presence of vibrationally impulsive internal conversion for the fastest reaction, RuRu in water. Extremely slow solvent dynamics are observed in the slow solvents despite a very short excited-state lifetime which indicates a solvent response outside the regime of linear response.

I. Introduction

A central goal in ultrafast condensed phase chemical dynamics is to obtain a molecular level picture of the nuclear and the electronic trajectories of reactive systems.[1−9] A unique and important opportunity to investigate such dynamics is found in ultrafast intramolecular electron-transfer reactions in solution. The reaction coordinate for electron-transfer reactions is comprised of both intramolecular nuclear (vibrational) coordinates and solvent nuclear degrees of freedom.[10−12] A particularly revealing prototype for ultrafast electron-transfer reactions is metal−metal charge-transfer reactions (MMCT), for which photoexcitation initiates the migration of an electron from one metal center to the other. Internal conversion from the excited state corresponds to the back electron-transfer reaction.

$$(NH_3)_5Ru^{III}NCRu^{II}(CN)_5^- \underset{ET}{\overset{h\nu}{\rightleftharpoons}} (NH_3)_5Ru^{II}NCRu^{III}(CN)_5^- \quad (1)$$

For photoinduced electron transfer reactions in which the reactant is optically prepared by excitation of the charge-transfer absorption of the "product" (as in eq 1), the nuclear degrees of freedom that are coupled to the electron-transfer reaction coordinate can also be investigated by static optical spectroscopy.[11,13−15] In particular, Raman spectroscopy in resonance with the MMCT band can be analyzed, in conjunction with the MMCT band-shape, to obtain quantitative information on the coupling of the electron-transfer process to the solvent coordinate and to specific vibration modes of the charge-transfer complex.

Another aspects of electron-transfer reaction dynamics that has been addressed is the role of vibrational dynamics and solvation dynamics in electron-transfer kinetics.[10,12,16,17] In early electron transfer models of the dynamic solvent effect, the reaction coordinate was assumed to be exclusively the solvent polarization, resulting in the prediction that the reaction rate should be inversely proportional to the longitudinal polarization relaxation time of the solvent. In these early studies the longitudinal polarization relaxation time was referred to diffusive solvation. Time resolved experiments on electron transfer have yielded rates that are significantly faster than the solvent longitudinal relaxation time.[15,18,19] Contemporary electron transfer theories are continuing to advance with the incorporation of such factors as a biphasic solvent response (including an inertial component of solvation and a slower diffusive solvation process) and ultrafast nonadiabatic internal conversion driven by intramolecular vibrational modes.[12,20−24] Barbara and coworkers[10] proposed a model of the dynamic solvent effect in solution phase electron transfer as a hybrid of the classical vibrational electron transfer theory of Sumi and Marcus and the vibronic electron transfer theory of Jortner and Bixon. The hybrid model was able to quantitatively treat the reaction rates

* To whom correspondence should be addressed. E-mail: p.barbara@mail.utexas.edu.

10.1021/jp002549q CCC: $19.00
Published on Web 10/19/2000

of various electron transfer reactions observed in a wide range of solvation time scales with the minimal number of solvent and intramolecular coordinates. In this model (as in Sumi/Marcus theory), classically broadened vibronic channels are introduced orthogonal to the classical solvent coordinate reducing the solvent dependence of the rate for slow solvents.

Ultrafast electron transfer reactions also provides an opportunity to investigate the kinetic consequences of ultrafast wave packet dynamics in a rapidly reacting systems far from equilibrium. Wave packet motion associated with solvation dynamics, and vibrational and electronic coherences are of particular interest.[4,6,8,25−29] Electron transfer reactions have been reported to proceed in a vibrationally coherent but electronically incoherent manner for a MMCT example.[8] In another electron-transfer reaction, the rate was observed to be modulated by vibrational coherence.[13] Slowly relaxing solvent, are particularly challenging in that they possess a broad range of time scales in their motions, ranging from hundreds of femtoseconds to hundreds of picoseconds.[30,31]

In this work we investigate the solvent dependence of the electron-transfer rate, vibrational coherence, stimulated emission, and the solvent motions displaced by back electron transfer using variable wavelength pump−probe spectroscopy of $(NH_3)_5$-$RuNCRu(CN)_5^-$ (RuRu) in formamide, ethylene glycol, and glycerol. These data are compared to previous experiments on RuRu in water.[32] We measure an electron-transfer time ($1/e$) of 220 fs for RuRu in ethylene glycol compared to a time of 100 fs in water. The observed solvent dependence of the electron-transfer time is consistent with theoretical predictions. The solvent dependent oscillations in the pump−probe signal reflect the coupling of the nuclear degrees of freedom of the solute to those of the solvent. The broad spectral coverage in both the pump and the probe wavelengths has allowed the observation of previously unobserved dynamics involving vibrational coherence and relaxing stimulated emission. The pump−probe data furthermore reflect the displacement of much slower solvent motions than should be accessible within linear response of independent solvent motions.

II. Experimental Section

The laser system used for the pump−probe experiment is composed of a home-built Kerr lens mode locked Ti:sapphire oscillator[33] pumped by Nd:YVO_4 laser and a Ti:sapphire multipass amplifier[34] pumped by Q-switched Nd:YLF laser. Briefly, <20 fs pulses centered at 800 nm generated from the oscillator, are stretched and amplified to produce ∼35 fs and 0.4 mJ pulses at 1 kHz, after recompression. The amplified femtosecond laser beam is divided into three beams. The first beam is used to pump an optical parametric amplifier (OPA), which is used to generate variable wavelength pump pulses. The pulses out of the OPA are compressed with an external fused silica prism pair to generate pulses of 15−25 fs duration, depending on the selected bandwidth. The second beam is used to pump the sample at 800 nm, and the third beam is used to generate white light continuum in a sapphire crystal, which is used as the probe pulse. The probe spectrum is pre-selected and compressed by a fused silica prism pair before it enters the sample. The compressed continuum pulses typically give pump−probe cross correlation times of 30−45 fs (fwhm). Throughout the experiment, the cross correlation time is maintained at ∼40 fs at all the pump and probe wavelengths.

The $(NH_3)_5RuNCRu(CN)_5^-$ (RuRu) sample solutions are rotated in a 1 mm thick rotating liquid cell with 200 μm fused silica windows, to avoid unwanted thermal effects from heating

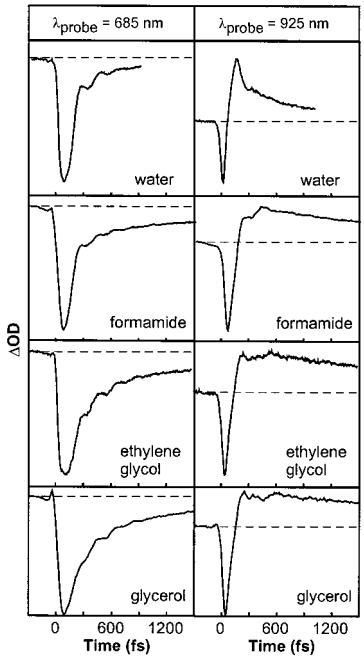

Figure 1. Pump-probe transient absorption data of RuRu in each solvent obtained with 800 nm pump.

of the sample by the pump pulse. The probe pulse energy is on the order of 1 nJ while the pump pulse is typically 10 μJ. The probe and pump beam waists are respectively, 50 and 300 μm fwhm. The polarization of the pump beam is set at magic angle relative to the probe, while the pump−probe crossing angle is 5 degrees at the sample position. To ensure that the transient absorption measurement is made in the linear regime of the photodepletion of the ground-state population, the pump pulse energy is maintained low enough so that less than 5% of the ground-state population is promoted to the excited state by the pump pulse. The transmitted probe beam is detected with Si or InSb photodiodes.

All the femtosecond absorption transients reported herein are corrected for a signal from the solvent by subtracting the neat solvent signal from the pump−probe signal of RuRu in solution. The solvent cross phase modulation artifact was scaled before subtraction to compensate for the attenuation of the pump intensity by the sample absorption. Both the solvent response as well as the transient absorption data were linear to pump intensity in the power regime used here. It was confirmed that the solvent response does not depend on the presence of the absorbing sample which might provide a spectral filtering effect.

III. Results

Overview of the Dynamics. The femtosecond absorption transients of RuRu in formamide, ethylene glycol and glycerol are compared to previously reported data in water,[32] at 800 pump/685 probe (800/685) and 800/925 in Figure 1. The transients in ethylene glycol at 800 and 615 nm pump and 600−1000 nm probe are shown in Figure 2. Table 1. contains the parameters of the multiexponential fits of the data. In each solvent, the transients show an initial instrument limited bleach which recovers on multiple time scales on the blue side of the static absorption spectra. There is variation between the solvents in the range of recovery times for the overall bleach recovery at the blue side of the static absorption spectra. The static absorption spectra peak at 685, 712, 732, and 762 nm in water, glycerol, ethylene glycol, and formamide, respectively, while the spectral widths are identical. Probing at the blue side of the

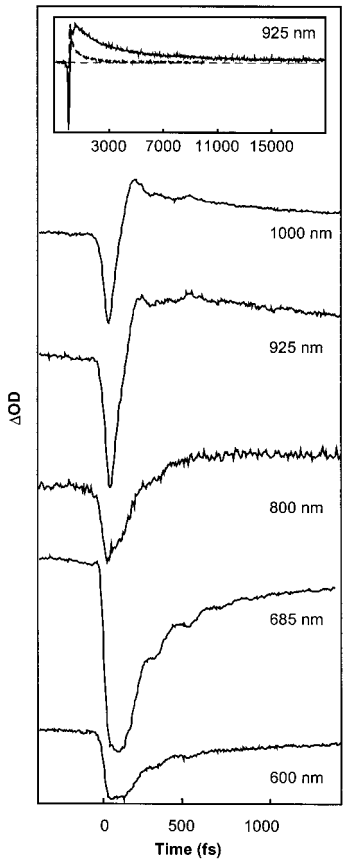

Figure 2. Pump−probe transient absorption data of RuRu in ethylene glycol obtained with 800 nm pump and variable wavelength probe. The transient at 800 nm probe was pumped at 615 nm. The inset shows a long time transient at 925 nm probe in ethylene glycol (solid line) and 910 nm probe in water (dashed line).

static absorption maxima highlights the overall similarities between ethylene glycol and glycerol at these probe wavelengths and the differences in time scales for the early time bleach recovery in water and formamide. The initial recovery in water and formamide is faster than in ethylene glycol and glycerol. The long time recovery, however, is fast only in water. Thus, formamide shows the greatest separation in time scales for the fast and slow components of the bleach recovery on the blue of the absorption spectrum. The solvation correlation function $S(t)$ in formamide also shows the most dramatic range in time scales.[30] Wavelengths further to the blue do not directly reflect population kinetics; the transient absorption spectroscopy in that spectral region also reflects ground-state desolvation (solvent relaxation to equilibrium for the electronic *ground* state) and vibrational relaxation.

On the red side of the static absorption spectra, the bleach recovers rapidly to an absorptive signal which decays on multiple, slower time scales. An absorptive signal suggests a hot ground-state population since there is no excited-state absorption in the probing window. In all solvents the bleach recovery is faster for probe wavelengths the further to the red. Probing at the red side of the static absorption maximum demonstrates that the decay time of the absorptive signal is similar in all solvents except water, whereas the magnitude of the bleach relative to the absorptive signal is quite different for all solvents. At the red probe wavelengths the absorptive signal decays on a 10 ps time scale in all solvents except water.

The effect of pump wavelength on the transients at 925 nm probing is presented in Figure 3. The transients have been normalized to the tail of the absorptive signal. Pumping at 615 nm shows differences from pumping at 800 nm. At 925 nm probe the amplitude of the bleach is diminished using 615 nm pump. The differences based upon pump wavelength are confined to the first 100 fs of the dynamics, while all subsequent dynamics are identical. While probing at 685 nm (not shown here), there is a sharp, additional negative ΔOD feature with 615 nm pump.

TABLE 1: Multiexponential Fitting Parameters for the Pump−Probe Transient Absorption Data of RuRu in Formamide, Ethylene Glycol, and Glycerol[a]

solvent	pump−probe (nm)	τ_1 (fs)	τ_2 (fs)	τ_3 (fs)	A_1	A_2	A_3
H_2O	800/570	150	2200		−0.78	−0.22	
	800/600	140	1980		−0.8	−0.2	
	800/685	125	1820		−0.95	−0.05	
	800/800[b]	85	880		−0.85	0.15	
	800/925	80	92	1140	−0.85[c]		0.15
	800/1000	67	80	1120	−0.93[c]		0.07
formamide	800/570	184	3742		−0.73	−0.27	
	800/600	155	3104		−0.75	−0.25	
	800/685	142	2808		−0.83	−0.17	
	800/925	107	597	4124	−0.90[c]		0.1
	800/1000	72	1166	9160	−0.95[c]		0.05
ethylene glycol	800/600	271	8884		−0.8	−0.2	
	800/685	257	10948		−0.84	−0.16	
	615/685	273	2159		−0.81	−0.19	
	615/800	220	4676		−0.77	0.23	
	800/925	107	1993	12330	−0.95[c]		0.05
	615/925	53	2081		−0.75	0.25	
	800/1000	63	1393	11791	−0.95[c]		0.05
glycerol	800/570	358	5039		−0.78	−0.22	
	800/600	331	3933		−0.78	−0.22	
	800/685	285	2715		−0.81	−0.19	
	800/925	82	1822	9875	−0.96[c]		0.04
	800/1000	50	1557		−0.88	0.12	

[a] The fitting function is $\Sigma A_n \exp(-t/\tau_n)$ and the amplitudes are normalized such that $\Sigma|A_n| = 1$. [b] Reference 8. [c] The amplitude is the sum of two amplitudes A_1 and A_2 having negative and positive amplitudes, respectively.

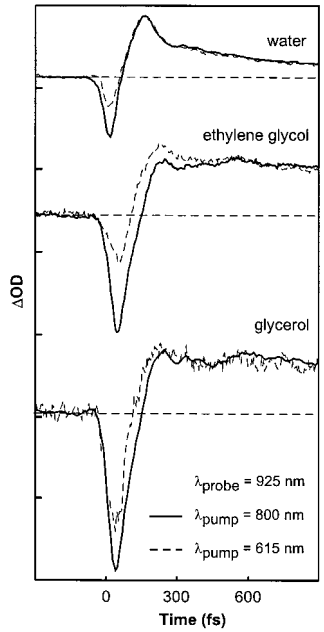

Figure 3. Pump−probe transient absorption data of RuRu in each solvent as a function of pump wavelength at 925 nm probe. The transients have been scaled to the absorptive signal.

The Time Zero ΔOD. At 800 nm pump, the time zero ΔOD amplitude does not scale with the absorption cross section. On

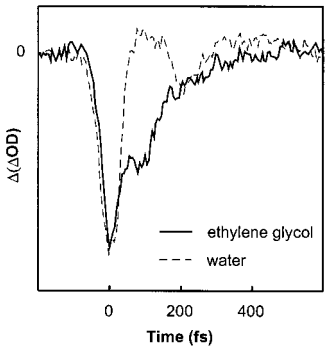

Figure 4. Pump−probe transient absorption data in which the 615 nm pump transient was subtracted from the 800 nm pump transient at a probe wavelength of 925 nm. The transients have been scaled as discussed in the text.

the red edge of the static absorption spectrum there, is an excess (compared to the static absorption spectrum) negative ΔOD component at early times for all solvents. In the Discussion section, the excess negative ΔOD component is assigned to stimulated emission from the an unrelaxed excited-state configuration of the solute−solvent system. Water[32] shows a smaller amount of excess negative ΔOD than ethylene glycol and glycerol. Glycerol in particular exhibits a large excess negative ΔOD component over a broad probe wavelength range, i.e., from 925 to 1050 nm.

The excess negative going ΔOD component at 925 nm probe is significantly attenuated when the pump wavelength is shifted from 800 to 615 nm, especially in ethylene glycol. The amplitude of this component also varies with solvent. In water, the time zero ΔOD ratio with 925 nm probing is 2:1 for 800 nm vs 615 nm pump wavelength compared-to-a ratio of 3:1 in ethylene glycol and 1.5:1 in glycerol. Figure 4 shows the shape of the extra, negative Δ*O*D at 925 probe in both ethylene glycol and water. Each trace, which we refer to as Δ(ΔOD), was determined by subtracting the 615 pump transient from the 800 nm pump transient at 925 nm probe for each solvent. Each transient was scaled to match the tail of the absorptive signal. The difference transient is instrument limited in water whereas it is asymmetric in ethylene glycol with a 100 fs decay time. Glycerol also has an asymmetric residual difference between the 800/925 and 615/925 data (not shown here).

The Residual Oscillations. The residual difference between the fits and the data, and the corresponding Fourier transforms for RuRu in each of the solvents, are shown in Figure 5 for 800 nm pumping and probing at 685 nm. These data exhibit an oscillatory intensity due to coherent vibrational motion in the ground state of the MMCT complex, as previously reported.[8,32,35] The data in Figure 5 show that the residual oscillations are solvent dependent. The amplitudes of the residuals and the power spectra have been normalized to the time zero ΔOD. Table 2 presents the solvent dependence of the oscillations. The only effect of pump wavelength in ethylene glycol at both 685 and 925 nm probe is that pumping at 615 nm attenuates the oscillations by a factor of 4. Figure 6 shows the residuals for RuRu in water at 800 nm pump over a broad range of probe wavelengths. The phase of the oscillations shows a $\pi/2$ (50 fs) phase shift from 1000 to 600 nm. A prominent peak is observed at 160 cm^{-1} in the power spectra in each of the solvents. In ethylene glycol and glycerol, an additional component at 85 cm^{-1} is resolved. This mode is also observed at both probe wavelengths using 615 nm pump in ethylene glycol. Linear predictive singular value decomposition (LPSVD) was used to obtain the dephasing time of the oscillations. The dephasing

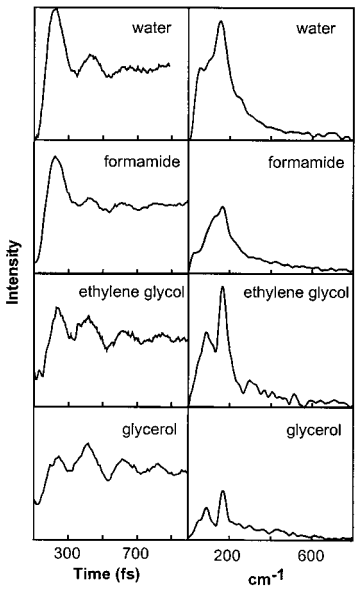

Figure 5. Residual difference between the fits of the transients and the data, and Fourier transforms of the residuals at 800 nm pump/685 nm probe in water, formamide, ethylene glycol and glycerol. The residuals were scaled to the bleach amplitude.

times (1/e) of the 160 cm^{-1} oscillations are 150, 150, 320, and 340 fs in water, formamide, ethylene glycol, and glycerol, respectively. The dephasing times of the 85 cm^{-1} oscillations are 380 and 330 fs in ethylene glycol and glycerol, respectively.

IV. Discussion

Solvent Dependence of the Electron-Transfer Rate. In a multicolor pump−probe experiment on a system with highly dynamic spectra, different probe wavelengths can produce widely different time scales in the transients, reflecting a distribution of molecular processes. Spectral shifting due to solvation on the excited state, as well as desolvation and vibrational cooling of the hot ground state can obscure the electronic population kinetics of interest. In an earlier paper we have shown that the time dependent integrated line shape provides the most accurate measure of population kinetics.[32] In the absence of a large number of probe wavelengths, however, an estimate for the ground state recovery dynamics can be obtained by monitoring at intermediate probe wavelength which have an absorption cross section that vary minimally during the ground state relaxation. In the RuRu/water system it was found that probing at 800 nm produces a bleach recovery time most closely resembling the recovery of the integrated absorption intensity.[32] Using the bleach recovery of the 615/800 data as a measure of population kinetics, we obtain an electron transfer time (1/e) of 220 fs of RuRu in ethylene glycol. This time is slightly faster than the previously reported value of 270 fs using 70 fs pulses at 792 nm.[15]

It is well-known that the electron-transfer rate is solvent dependent in a complex manner. Both the solvent coordinate as well as intramolecular nuclear vibrational coordinates can act as promoting modes for electron transfer. On the basis of the classical vibrational theory of Sumi and Marcus[17] and the vibronic theory of Jortner and Bixon,[36] Barbara and co-workers proposed a minimal model which was able to predict the dynamic solvent effect on electron-transfer rates in a wide range of solvents[10] and over a broad range of reaction free energies. This "hybrid" model showed that the electron transfer time should increase with solvation time for fast solvents but then

TABLE 2: Solvent Dependence of Oscillation Amplitude[a]

solvent	A_{685}	A_{925}	OD_{max} (nm)	OD_{685}[b]	OD_{925}[b]	$dOD_{685}/d\omega$ (OD/cm^{-1})	$dOD_{925}/d\omega$ OD/cm^{-1})	dephasing time[c] (fs)
H_2O	0.34	0.32	685	1.00	0.13	0.01	0.36	150
formamide	0.26	0.18	762	0.76	0.48	0.87	0.94	150
ethylene glycol	0.18	0.11	732	0.88	0.28	0.70	0.73	320
glycerol	0.16	0.11	712	0.95	0.18	0.46	0.57	340

[a] Peak to peak oscillation amplitude relative to bleach amplitude. [b] OD relative to absorption maximum. $OD_{max} = 3000\ M^{-1}\ cm^{-1}$. [c] LPSVD analysis of the 160 cm^{-1} mode.

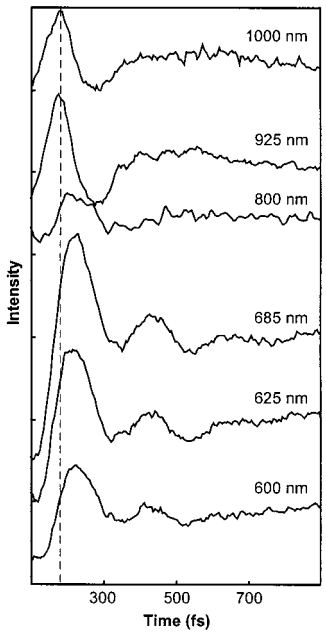

Figure 6. Residual difference between the fits of the transients and the data of the transients at 800 nm pump as a function of probe wavelength in water. The dashed line illustrates the phase shift in the oscillations.

weaken in its solvent dependence as the solvation times become slower, due to an interplay between solvation dynamics and vibronically controlled internal. There is a crossover from dynamic solvent controlled electron transfer kinetics in fast solvents to vibrationally controlled electron-transfer kinetics in slow solvents conversion (as in the Sumi−Marcus model).

For ultrafast electron transfer in RuRu in water, there is some evidence for dynamic solvent control of the ET kinetics. RuRu in water has an electron-transfer time of 100 fs whereas ethylene glycol produces a time of 220 fs. These times may be compared to the solvation times from transient Stokes shift experiments in which water[37] has times of 50, 180, and 880 fs while ethylene glycol[30] has times of 187, 5000, and 32000 fs. The ultrafast component in water has been assigned to inertial solvation whereas the nature of the ultrafast component in ethylene glycol has not been established to our knowledge. The slower dynamics are widely believed to be diffusive in nature. The slower electron transfer time in ethylene glycol is apparently a dynamic solvent effect. Furthermore, in ethylene glycol the electron-transfer time is faster than the solvation diffusional time scales demonstrating that the reaction is promoted by inertial solvent degrees of freedom and/or vibrational solute degrees of freedom in this solvent. Electron-transfer times faster than diffusional solvation have been observed in other systems as well.[18,19] However, the lack of a direct correspondence of the electron-transfer time with the inertial solvent time scales, suggests that vibronic factors must also be important in controlling the ET rate. [12]

The absence of a pump wavelength dependence of the dynamics after 100 fs indicates that the electron-transfer rate is not sensitive to the *initial* excess vibrational energy in the excited state. An assumption of the hybrid model is that the vibrational relaxation rate is faster than the electron-transfer rate,[10,18] and correspondingly, the initial excess vibrational energy is assumed to be rapidly dissipated in this theory. However, it is unlikely that this is the correct explanation for the lack of dependence of the electron transfer rate on initial excess vibrational energy since other data (see below) suggests that the time scale for vibrational relaxation in the excited state is in fact comparable or even slower than the electron transfer time scale for the relevant vibrational modes. Thus, the data suggest that the electron transfer rate is not strongly dependent on the *instantaneous* excess vibrational energy not just the initial excess vibrational energy.

Vibrational Coherences. Oscillatory vibrational wave packet dynamics have been observed in many systems.[1,3−5,8,9,25−27,38] Such behavior is typically associated with resonant impulsive stimulated Raman scattering (RISRS) and/or excited-state wave packet motion. The role of excited-state wave packet motion is simplified in the MMCT case as the excited-state lifetime is less than or equal to a single vibrational period, depending on the solvent. In the RISRS mechanism Franck−Condon allowed vibrational coherences are excited that lie within the pump bandwidth.[38−40] Oscillatory behavior was previously observed for RuRu in water and has been assigned to RISRS.[8] This coherence modulates the dynamic absorption spectrum resulting in oscillatory behavior for single wavelength transients. The Fourier power spectra of the residual oscillations in a RISRS signal exhibits vibrational peaks that correspond to Raman active modes in the conventional resonance Raman spectrum. Theory shows, however, that there is no simple relation, between the amplitude of the oscillations in the RISRS experiment and the corresponding amplitude in a conventional resonance Raman experiment.[26,39,40]

Conventional resonance Raman spectroscopy of RuRu in solution phase has provided relative resonance Raman cross sections of several intramolecular modes for RuRu. These cross sections which have been analyzed to determine Franck−Condon factors, and correspondingly, vibrational reorganization energies for the various vibrational modes.[41,42] There are several modes in the 300−500 cm^{-1} range with large Raman activity. An additional mode at low frequency, i.e., 160 cm^{-1}, with a relatively large cross-section was recently observed.[42] Due to the large Rayleigh background, however, resonance Raman spectroscopy cannot accurately measure the peak intensity of the 160 cm^{-1} band.

The amplitudes of the vibrational peaks in Fourier power spectra of the residual oscillations in water deviates more strongly from the low-frequency resonance Raman spectra[35,41−43] of this compound than has been typically observed for large polyatomics,[26,27,38,39] suggesting that the observed effects are more complex than the usual RISRS mechanism. Table 3. presents the relative amplitudes of the low-frequency peaks in the resonance Raman[42] and the RISRS[35] experiments. The present experiment was not able to distinctly resolve peaks

TABLE 3: Resonance Raman[a] and RISRS[b] Peak Areas

frequency[a] (cm^{-1})	A_{RR}	A_{RISRS}
160	1.00	1.00
263	0.85	
351	0.05	
492	0.80	0.08
535	0.13	
566	0.67	0.03

[a] Reference 42. [b] Reference 35.

higher in frequency than the 160 cm^{-1} mode.[43] With improved signal-to-noise levels, Scherer and co-workers were able to resolve two small amplitude, higher frequency modes.[35] Another indication that the usual RISRS mechanism cannot account adequately for the observed vibrationally coherent data for RuRu is found in the probe wavelength dependence of the data (Table 2). The usual dependence of the RISRS signal upon probe wavelength has been well established.[26,40] Oscillations are strongest at points in the static absorption spectrum which have the greatest slope. At the probe wavelengths analyzed for formamide, ethylene glycol and glycerol, the slope of the static absorption spectrum is nearly the same. Consistent with the RISRS picture, the amplitude of the oscillations is nearly equal at the two probe wavelengths of 685 and 925 nm as well. The oscillations in water, however, are anomalous with respect to the standard RISRS picture in that the amplitude of the oscillations is large at 685 nm where the slope of the absorption spectrum is smallest. Furthermore, the expected trends in the phase shift for the vibrational coherences in RISRS at probe wavelengths within either the red or the blue of the absorption maximum is absent for RuRu. There is, however a $\pi/2$ rad (50 fs) phase shift upon going from the red side to the blue side, rather than the expected π phase shift. While there is some similarity to conventional Franck−Condon allowed RISRS, the difference suggests interference by large amplitude non-Condon effects.[32] In addition to the spectral peak oscillations observed in the wavelength resolved experiments, spectral intensity oscillations have been observed in a wavelength integrated analysis.[32] Unfortunately, the absence of a theoretical framework with which to describe non-Condon RISRS precludes the possibility of a definitive assignment.

Another potential source for RuRu of deviations from the usual RISRS mechanism is associated with the ultrafast internal conversion process. In a rapidly reacting system like RuRu in water, which has an ET time of less than 100 fs, the internal conversion itself can be in the vibrationally impulsive regime. In analogy to electronic excited state wave packet motion, the production of ground state population occurs more rapidly than a vibrational period. In slow solvents such as ethylene glycol, however, a 220 fs internal conversion is not vibrationally impulsive for a mode with a 200 fs period. Table 2. shows that the oscillation amplitudes are larger in the faster solvents, water and formamide, without correlation to either slope or OD of the spectra. Faster solvents should furthermore produce smaller oscillation amplitudes based upon an decreased electronic dephasing time.[38] On the basis of these observations, we suggest that the RISRS mechanism is active in all solvents while the faster solvents have ground state wave packet motion that is supplemented by the additional mechanism of vibrationally impulsive internal conversion.

We also have investigated in detail the solvent dependence of the dephasing time of the vibrational coherences. The observed trends are consistent with previous RISRS work.[38] In RuRu, the dephasing time increases by a factor of 2 from the more polar and quickly relaxing solvents (water and formamide) to the slower, less polar solvents (ethylene glycol and glycerol). Furthermore, the trend in the solvent dependence of the vibrational dephasing times suggests an interpretation of the nonoscillatory 1−2 ps time scale spectral dynamics found for RuRu in all solvents. The variation of the time scale for this component with solvent parallels the variation in dephasing times. Water has 1 ps components at the red of the absorption maximum whereas ethylene glycol has a 2 ps component. We, therefore, assign the nonoscillatory dynamics on the 1−2 ps time scale to vibrational population relaxation on the ground electronic state in the slower solvents. Since these time scales also correspond to diffusional solvation in water,[37] it is not possible to separate solvation from vibrational relaxation[32] in the overall spectral dynamics for this solvent.

The vibrational relaxation time was measured for the terminal CN stretching mode for RuRu in water using infrared spectroscopy. The time scale of the vibrational relaxation of this mode was found to be 0.5−6 ps using 2 ps pulses.[44] In an analogous system where one of the Ru atoms is replaced with Fe, the bridging CN stretching mode showed a relaxation time of 1.3 ps in D_2O using 200 fs pulses.[7] These experiments may lack time resolution to probe the early time dynamics so may not be probing the early time vibrationally hot ground state we observed in these 40 fs resolved experiments and furthermore may not be probing the same vibrational transitions responsible for the apparent cooling of the dynamic spectrum at early time.

Stimulated Emission. At early time in a pump−probe signal, there are additional contributions from both stimulated emission and coherent coupling.[28,40] The differences in the early time signal for RuRu in each of the solvents should, in part, reflect differences in both the coherent coupling and the stimulated emission contributions to the total signal. Pumping at different wavelengths allows us to discriminate against coherent coupling. It is unlikely that coherent coupling is the origin of the excess negative ΔOD component in the present experiment due to three factors: (i) the larger than 2500 cm^{-1} of pump−probe detuning which tends to diminish coherent pump−probe coupling: (ii) the large vibrational reorganization energy which tends to increase the electronic dephasing rate through vibrational contributions[29] and (iii) the observation that the excess negative ΔOD signal in ethylene glycol and glycerol is present well after the pump and probe are temporally separated. We therefore assign the extra, negative ΔOD component to stimulated emission.[32]

The stimulated emission appears short-lived due to partial cancellation by hot ground-state absorption, spectral shifting out of the probe window by excited-state solvation, and possible non-Condon effects.[32] Spectral simulations show that when low frequency modes are coherently excited, the emission is initially sharp and intense and subsequently becomes broader and reduces in amplitude due to vibrational dephasing and relaxation.[32,45] Since the emission occurs prior to vibrational relaxation, pumping at 615 nm will reduce the emission intensity at long wavelengths such as 1000 nm. At an individual wavelength, the emissive component will attenuate more rapidly than the excited state lifetime due to shifting out of the probe window by solvation and by spectral spreading due to vibrational dephasing. Since the dephasing and relaxation rates are solvent dependent, attenuation of emission by spectral spreading and solvation, should be slower in the slower solvents as is experimentally observed. Because of the number of processes active in the evolution of the stimulated emission there is no simple picture which may describe the solvent dependence of the unrelaxed stimulated emission.

Displacement of Slow Solvent Modes by a Fast Perturbation. While each of the solvents exhibit dynamics on the 1−2 ps time scale due to vibrational population relaxation, only the alcohols and formamide have dynamics on the 10 ps time scale. This observation suggests that these slow dynamics are solvent related. Although the alcohols and formamide each have components in S(t) on the tens of picosecond time scale or longer,[30] these modes should not be displaced during an excite state lifetime of 220 fs. To demonstrate that slow solvent modes should not be displaced, we simulated the diffusion of a Boltzmann population distribution along a classical harmonic potential. The parameters in the model are the solvent reorganization energy (4000 cm^{-1}) partitioned by the S(t) amplitudes, with the relaxation times given by S(t).[30] The slow modes should have amplitudes of no more than a few percent of the amplitudes found in the S(t). The simulations quantify the idea that slow solvent motions should not be displaced during a short excited-state lifetime within the linear response approximation for the solvent motions.

Because of the large total reorganization energy of ca. 6000 cm^{-1}, there is a great deal of energy disposal into the solvent coordinate.[15] This energy disposal will locally heat the solute's environment which may result in long time dynamics as the local temperature equilibrates. The effect of local heating of the solvent can be calculated with a heat diffusion model and the temperature dependence of the absorption spectra in each solvent.[15,46] A locally hot environment will produce a redshifted absorption. On the basis of the heat capacities, thermal diffusion constants, and temperature dependences of water and ethylene glycol, we find that RuRu in ethylene glycol does have a more locally heated environment than water at 5 ps. But the effect of local heating on the positive ΔOD is around one percent of the overall hot ground-state signal. We can therefore rule out local heating of the solvent as the source of the slow, 10 ps dynamics in the alcohols.

Since ideal solvation probes have long lifetimes, little is known about the solvation dynamics of systems in which the exited state lifetime is very short. The question naturally arises as to how slow solvent motions are displaced when the solvent has time only to respond on a hundred femtosecond time scale. Since RuRu has such a large reorganization energy, one may consider the validity of linear response in this system due to the very large change in charge distribution upon excitation. The change in dipole moment for RuRu is 13 D[47] while C153 is has a change of 8 D.[30] The change in dipole moment is not overwhelmingly greater than for C153. Furthermore, theory has shown that linear response is qualitatively and even semiquantitatively accurate for very severe changes in charge distribution such as ionization or neutralization reactions of atomic solutes.[31] Based simply upon the change in dipole moment and solvent reorganization of RuRu in these solvents, it is reasonable to expect that linear response should be applicable. Simulations are needed to verify whether this system is in the linear or nonlinear regime of solvent response.

The presence of specific solute−solvent interactions such as hydrogen bonding can complicate solvation dynamics.[48−51] It is possible that the slowest time scale solvent dynamics observed have to do with the scrambling of the hydrogen bonding network as the electron-transfer reaction proceeds.[52] An alternative mechanism of slow mode displacement may involve coupling between solvent modes. Fast solvent motions may cascade into slower motions. The interaction of intermolecular and intramolecular modes in neat solvents has been the topic of mode coupling.[53] The coupling of solvent modes has been experimentally investigated through multidimensional nonlinear spectroscopy such as fifth-order two-dimensional Raman.[54,55] While it is still unclear whether there is direct experimental evidence for such mode coupling processes,[56] our observation of displacement of slow modes by a fast perturbation suggests solvent mode coupling as a possibility. In systems for which there are a broad range of time scales for motions, there may be a cascading of energy from fast modes to slow modes. While we do see evidence for the displacement of slow solvent motions by a fast perturbation, the data do not allow an unambiguous assignment of the origin of the process.

V. Conclusions

In this work we have performed a multiccolor femtosecond pump−probe investigation of intervalence electron transfer of RuRu in water, formamide, ethylene glycol and glycerol. The use of multiple pump and probe wavelengths which span the red and the blue sides of the static absorption spectra has provided a detailed picture of the electron transfer kinetics, solvation dynamics, as well as vibrational coherence and relaxation. We find an electron transfer time of 220 fs for RuRu in ethylene glycol compared to an electron transfer time of 100 fs of RuRu in water. The somewhat slower rates observed in the much slower relaxing solvents are qualitatively consistent with the hybrid model for electron transfer.

Vibrational coherence is maintained during electron transfer by production of wave packet motion on the ground electronic state by resonant impulsive stimulated Raman scattering. The power spectra of the residuals suggests that the majority of the intramolecular reorganization energy comes from a low frequency, 160 cm^{-1} Raman active mode. The oscillations show differences from Franck−Condon allowed RISRS indicating non-Condon contributions to the RISRS cross section as well as vibrationally impulsive internal conversion for RuRu in water. We observe solvent dependent vibrational dephasing and population relaxation rates which further affect the behavior of the relaxing stimulated emission. This system has also revealed interesting solvation dynamics on the ground electronic state following back electron transfer. Despite the short excited-state lifetime of around 220 fs, slow solvent modes were observed in some solvents. This observation of slow solvent motions in response to a very short excited-state lifetime may be indicative of either breakdown of linear response, or indication of the coupling of solvent motions. The present experiments are not able to distinguish the origin of the slow solvent motions.

Acknowledgment. We gratefully acknowledge support of this research by the Basic Energy Sciences Program of the Department of energy and the Robert A. Welch Foundation.

References and Notes

(1) Wurzer, A. J.; Wilhelm, T.; Piel, J.; Riedle, E. *Chem. Phys. Lett.* **1999**, *299*, 296.

(2) Haran, G.; Morlino, E. A.; Matthes, J.; Callender, R. H.; Hochstrasser, R. M. *J. Phys. Chem. A* **1999**, *203*, 2202.

(3) Hess, S.; Bursing, H.; Vohringer, P. *J. Chem. Phys.* **1999**, *111*, 5461.

(4) Sporlein, S.; Zinth, W.; Wachtveitl, J. *J. Phys. Chem. B* **1998**, *102*, 7492.

(5) Arnett, D. C.; Moser, C. C.; Dutton, P. L.; Scherer, N. F. *J. Phys. Chem. B* **1999**, *103*, 2014.

(6) Wynne, K.; Reid, G. D.; Hochstrasser, R. M. *J. Chem. Phys.* **1996**, *106*, 2287.

(7) Wang, C.; Mohney, B. K.; Akhremitchev, B. B.; Walker, G. C. *J. Phys. Chem. A* **2000**, *104*, 4313.

(8) Reid, P. J.; Silva, C.; Barbara, P. F.; Karki, L.; Hupp, J. T. *J. Phys. Chem.* **1995**, *99*, 2609.

(9) Arnett, D. C.; Vohringer, P.; Scherer, N. F. *J. Am. Chem. Soc.* **1995**, *117*, 12262.
(10) Barbara, P. F.; Walker, G. C.; Smith, T. P. *Science* **1992**, *256*, 975.
(11) Barbara, P. F.; Meyer, T. J.; Ratner, M. A. *J. Phys. Chem.* **1996**, *100*, 13148.
(12) Bagchi, B.; Gayathri, N. *Adv. Chem. Phys.* **1999**, *107*, 1.
(13) Wynne, K.; Hochstrasser, R. M. *Adv. Chem. Phys.* **1999**, *107*, 263.
(14) Walker, G. C.; Barbara, P. F.; Doorn, S. K.; Dong, Y.; Hupp, J. T. *J. Phys. Chem.* **1991**, *95*, 5712.
(15) Tominaga, K.; Kliner, D. A. V.; Johnson, A. E.; Levinger, N. E.; Barbara, P. F. *J. Chem. Phys.* **1993**, *96*, 1228.
(16) Jortner, J.; Bixon, M. *J. Chem. Phys.* **1988**, *88*, 167.
(17) Sumi, H.; Marcus, R. A. *J. Chem. Phys.* **1986**, *84*, 4894.
(18) Walker, G. C.; Åkesson, E.; Johnson, A. E.; Levinger, N. E.; Barbara, P. F. *J. Phys. Chem.* **1992**, *96*, 3728.
(19) Nagasawa, Y.; Yartsev, A. P.; Tominaga, K.; Johnson, A. E.; Yoshihara, K. *J. Chem. Phys.* **1994**, *101*, 5717.
(20) Wolfseder, B.; Seidner, L.; Stock, G.; Domcke, W. *Chem. Phys. Lett.* **1997**, *217*, 275.
(21) Muller, U.; Stock, G. *J. Chem. Phys.* **1997**, *107*, 6230.
(22) Bixon, M.; Jortner, J. *J. Chem. Phys.* **1997**, *107*, 1470.
(23) Stuchebrukhov, A. A.; Song, X. *J. Chem. Phys.* **1994**, *101*, 9354.
(24) Evans, D. G.; Nitzan, A.; Ratner, M. A. *J. Chem. Phys.* **1998**, *108*, 6387.
(25) Ashworth, S. H.; Hasche, T.; Woerner, M.; Reidle, E.; Elsaesser, T. *J. Chem. Phys.* **1996**, *104*, 5761.
(26) Yang, T. S.; Chang, M. S.; Chang, R.; Hayashi, M.; Lin, S. H.; Vohringer, P.; W, W. D.; Scherer, N. F. *J. Chem. Phys.* **1999**, *110*, 12070.
(27) Bardeen, C. J.; Wang, Q.; Shank, C. V. *J. Phys. Chem. A* **1998**, *102*.
(28) Cong, P.; Yan, Y. J.; Deuel, H. P.; Simon, J. D. *J. Phys. Chem.* **1994**, *100*, 7855.
(29) Book, L. D.; Scherer, N. F. *J. Chem. Phys.* **1999**, *111*, 792.
(30) Horng, M. L.; Gardecki, J. A.; Papazyan, A.; Maroncelli, M. *J. Phys. Chem.* **1995**, *99*, 17311.
(31) Stratt, R. M.; Maroncelli, M. *J. Phys. Chem.* **1996**, *100*, 12981.
(32) Son, D. H.; Kambhampati, P.; Kee, T. W.; Barbara, P. F. *J. Chem. Phys.* **2000**. Submitted for publication.
(33) Asaki, M. T.; Huang, C. P.; Garvey, D.; Zhou, J.; Murnane, M. M.; Kapteyn, H. C. *Opt. Lett.* **1993**, *18*, 977.
(34) Backus, S.; Peatross, J.; Huang, C. P.; Kapteyn, H. C.; Murnane, M. M. *Opt. Lett.* **1995**, *20*, 2000.
(35) Scherer, N. F. Private communication.
(36) Jortner, J.; Bixon, M. *J. Chem. Phys.* **1988**, *88*, 167.
(37) Jimenez, R.; Fleming, G. R.; Kumar, P. V.; Maroncelli, M. *Nature* **1994**, *369*, 471.
(38) Banin, U.; Bartana, A.; Ruhman, S.; Kosloff, R. *J. Chem. Phys.* **1994**, *101*, 8461.
(39) Johnson, A. E.; Myers, A. B. *J. Chem. Phys.* **1996**, *104*, 2497.
(40) Pollard, W. T.; Mathies, R. A. *Annu. Rev. Phys. Chem.* **1992**, *43*, 497.
(41) Doorn, S. K.; Hupp, J. T. *J. Am. Chem. Soc.* **1989**, *111*, 1142.
(42) Bignozzi, C. A.; Argazzi, R.; Strouse, G. F.; Schoonover, J. R. *Inorganica Chimica Acta* **1998**, *275*, 380.
(43) The coherent bandwidth of the pump was independently confirmed using a standard RISRS system, Nile blue in methanol. In this system at 615/685, we were able to observe oscillations past 800 cm^{-1} demonstrating that if the 500 cm^{-1} modes had sufficiently large reorganization energy, they should be observable.
(44) Doorn, S. K.; Dyer, R. B.; Stoutland, P. O.; Woodruff, W. H. *J. Am. Chem. Soc.* **1993**, *115*, 6398.
(45) Lin, S. H.; Fain, B.; Hamer, N. *Adv. Chem. Phys.* **1990**, *79*, 133.
(46) Dong, Y.; Hupp, J. T. *Inorg. Chem.* **1991**, *31*, 3322.
(47) Vance, F. W.; Karki, L.; Reigle, J. K.; Hupp, J. T.; Ratner, M. A. *J. Phys. Chem. A* **1998**, *102*, 8320.
(48) Sese, G.; Pardo, J. A. *J. Chem. Phys.* **1998**, *108*, 6347.
(49) Yu, J.; Berg, M. *Chem. Phys. Lett.* **1993**, *208*, 315.
(50) Chapman, C. F.; Fee, R. S.; Maroncelli, M. *J. Phys. Chem.* **1995**, *99*, 4811.
(51) Chudoba, C.; Nibbering, E. T. J.; Elsaesser, T. *Phys. Rev. Lett.* **1998**, *81*, 3010.
(52) Reid, P. J.; Barbara, P. F. *J. Phys. Chem.* **1995**, *99*, 3554.
(53) Okumura, K.; Tanimura, Y. *J. Chem. Phys.* **1997**, *107*, 2267.
(54) Steffen, T.; Duppen, K. *Chem. Phys. Lett.* **1998**, *290*, 229.
(55) Tokmakoff, A.; Lang, M. J.; Larsen, D. S.; Fleming, G. R.; Chernyak, V.; Mukamel, S. *Phys. Rev. Lett.* **1997**, *79*, 2702.
(56) Blank, D. A.; Kaufman, L. J.; Fleming, G. R. *J. Chem. Phys.* **1999**, *111*, 3105.